Determination of Base Pairing in Ribonucleic Acid by Fourier-Transform Infrared Spectrometry: Yeast Ribosomal 5S Ribonucleic Acid†

Kent O. Burkey, Alan G. Marshall,* and James O. Alben*

ABSTRACT: Fourier-transform infrared (FT-IR) spectra of yeast ribosomal 5S RNA have been acquired at several temperatures between 30 and 90 °C. The difference spectrum between 90 (bases unstacked) and 30 °C (bases stacked) provides a measure of base stacking in the RNA. Calibration difference spectra corresponding to stacking of G-C or A-U pairs are obtained from "reference" FT-IR spectra of poly(rG)·poly(rC) minus 5′-GMP and 5′-CMP or poly(rA)·poly(rU) minus 5′-AMP and 5′-UMP. The best fit linear combination of the calibration G-C and A-U difference spectra to the 5S RNA (90 − 30 °C) difference spectrum leads to a total of 25 ± 3 base pairs (17 G-C pairs + 8 A-U pairs) for the native yeast 5S RNA in the absence of Mg^{2+}. In the presence of Mg^{2+}, an additional six base pairs are detected by FT-IR (one G-C and five A-U). FT-IR melting curve midpoints show that A-U and G-C pairs melt together (65 and 63 °C) in the presence of Mg^{2+} but A-U pairs melt before G-C pairs (47 vs. 54 °C) in the absence of Mg^{2+}.

One 5S RNA molecule is a required constituent for protein synthesis in virtually every studied prokaryotic or eukaryotic ribosome (Erdmann, 1976). The primary nucleotide sequences of more than 50 5S RNAs have been determined (Erdmann, 1982). Because of the apparent universal function of 5S RNA, it is widely speculated that all 5S RNAs share a common secondary structure. (For example, reconstitution of 5S RNA from one prokaryote with the remaining ribosomal components from a different prokaryote leads to functional ribosomes.) Thus, the determination of a 5S RNA secondary structure for even a single species would have broad implications for 5S RNA structure in other species.

Although a "cloverleaf" secondary structure is universally accepted for all known transfer RNAs, there is as yet no agreement on a universal secondary structure for any of the larger RNAs. For ribosomal 5S RNA, for example, literally dozens of secondary structures have been proposed (Erdmann, 1976; Appel et al., 1979).

Secondary structure is generally deduced from two complementary types of experiments. The first type (e.g., nuclease cleavage, chemical modification, oligonucleotide binding) typically identifies *single*-stranded bases or segments. The second type (e.g., differential scanning microcalorimetry and ^1H Fourier-transform nuclear magnetic resonance, infrared, Raman, and ultraviolet spectrometry) counts and identifies *paired* or *stacked* bases. In addition, the gross shape of the macromolecule can be guessed from light scattering, low-angle X-ray scattering, and circular dichroism (CD) measurements. For 5S RNAs, most published experiments are of the first type. Only recently have the spectroscopic techniques begun to be applied to 5S RNAs.

Although UV spectra of polynucleotides are sensitive to base stacking, analysis for the proportion of individual base-pair types (e.g., G-C vs. A-U vs. G-U) can be obscured by the high degree of overlap between spectra for each of the various bases or base pairs. As noted in a recent review (Carey, 1982), Raman and infrared spectra share the advantage that bands associated with individual bases (A, G, C, U) are at least partly resolved. For example, Raman spectra provided some of the best early evidence for base-pair composition and ratio in 5S RNA from *Escherichia coli* (Luoma & Marshall, 1978a; Chen et al., 1978) and yeast (Luoma & Marshall, 1978b).

Attempts to determine base-pair composition for 5S RNA from infrared spectra have not been as successful. For *E. coli* 5S RNA, for example, totals of 41 or 56 base pairs were deduced from infrared data (Richards et al., 1972; Appel et al., 1979), whereas subsequent proton Fourier-transform nuclear magnetic resonance (FT-NMR) spectra (Burns et al., 1980) suggested about 33. The proton NMR data are especially credible, since similar measurements for yeast $tRNA^{Phe}$ gave 26 ± 1 base pairs (Reid & Robillard, 1975), in precise agreement with the X-ray diffraction values for two different crystal forms of that molecule (Ladner et al., 1975; Sussmann & Kim, 1976). For yeast (*Saccharomyces carlsbergensis*) 5S RNA, infrared results were interpeted to give a total of 46 base pairs (Stulz et al., 1981), again greatly exceeding the ^1H FT-NMR value of 32 for 5S RNA from another yeast (*Saccharomyces cerevisiae*) of identical primary nucleotide sequence (Luoma et al., 1980).

A more recent and more accurate infrared determination gave 33 base pairs for *E. coli* 5S RNA (Böhm et al., 1981); the improvement was ascribed to more accurate base-line compensation for solvent (D_2O and HDO). It is true that strong absorption by the solvent leads to noisy and imprecise background ("base line") in the IR difference spectra from which the weak RNA absorption bands are measured. [Although the problem must have been obvious in the original IR spectra, it cannot be seen in any of the "smoothed" published spectra (Richards et al., 1972; Appel et al., 1979; Stulz et al., 1981; Böhm et al., 1981).] However, a more important improvement may be that Böhm et al. base their simulations on an RNA *difference* spectrum, $\epsilon_{RNA}(95\ °C) - \epsilon_{RNA}(20\ °C)$, rather than an RNA extinction spectrum at a *single* temperature (Richards et al., 1972; Appel et al., 1979; Stulz et al., 1981). Since the IR absorbance of RNA, even at 90 °C, is smaller at all wavelengths (1400–1700 cm^{-1}) than the summed spectra of its component mononucleotides, any attempt to simulate the RNA IR spectrum at just one temperature will overestimate the apparent number of paired bases, since the reduced intensity in RNA compared to mononucleotides will be interpreted as additional base pairs. However, a difference measurement, $\epsilon_{RNA}(90\ °C) - \epsilon_{RNA}(30$

† From the Department of Chemistry (K.O.B. and A.G.M.), the Department of Biochemistry (A.G.M.), and the Department of Physiological Chemistry (J.O.A.), The Ohio State University, Columbus, Ohio 43210. *Received February 22, 1983.* This work was supported by U.S. Public Health Service Grants to J.O.A. (NIH 1R01-HL-17839 and HL-28144) and A.G.M. (NIH 1R01-GM-29274).

0006-2960/83/0422-4223$01.50/0

°C), should remove that intensity discrepancy, leaving an RNA difference spectrum that more accurately reflects base pairing.

The high dynamic range, signal-averaging capability, and facility for digitized data manipulation (filtering, base-line correction, difference spectra) of Fourier-transform infrared (FT-IR) spectrometry provide major advantages over the dispersive IR instruments from which all published IR spectra of 5S RNA have been obtained. In the present paper, FT-IR spectra from yeast 5S RNA at various temperatures are compared to FT-IR spectra of paired and unpaired ribonucleotides. The results can then be analyzed to yield reliable estimates for the numbers of G-C and A-U base pairs in the 5S RNA.

Theory

Thomas (1969) and Schernau & Ackerman (1977) have developed a relation between the absorbance of the aromatic bases of RNA in the mid-infrared region and the base-pair composition of the RNA. The method is based on the increase in IR absorption observed on unstacking of the bases (as by increase in temperature) and an assumed correspondence between base stacking and base pairing (see Discussion).

The method begins by supposing that each of the four ribonucleotides can assume only stacked (s) or unstacked (u) states. It is further assumed that all stacked bases are paired and that all base pairs are either A-U or G-C (e.g., no G-U pairs). Let $\epsilon(\nu)_{i,s}$ and $\epsilon(\nu)_{i,u}$ be the respective molar extinction coefficients at ν of base i in the stacked and unstacked states. $\epsilon(\nu)_{A,u}$, $\epsilon(\nu)_{U,u}$, $\epsilon(\nu)_{G,u}$, and $\epsilon(\nu)_{C,u}$ can be determined experimentally from spectra of the mononucleotide 5′-phosphates. $\epsilon(\nu)_{A,s}$ and $\epsilon(\nu)_{U,s}$ cannot be measured separately, but their sum can be determined from a spectrum of poly(rA)·poly(rU), from which

$$\epsilon(\nu)_{A\text{-}U} = (1/2)[\epsilon(\nu)_{A,s} + \epsilon(\nu)_{U,s}] \quad (1)$$

Similarly, from a spectrum of poly(rG)·poly(rC)

$$\epsilon(\nu)_{G\text{-}C} = (1/2)[\epsilon(\nu)_{G,s} + \epsilon(\nu)_{C,s}] \quad (2)$$

Finally, if all base pairs are "melted" (i.e., unstacked) at 90 °C and all base pairs are present at 30 °C, then

$$\frac{\epsilon(\nu)_{RNA,90°C} - \epsilon(\nu)_{RNA,30°C}}{2\alpha} = f_{A,s} + \frac{\beta}{\alpha} f_{G,s} \quad (3)$$

where α is defined as the normalized (per mole of phosphate) absorbance difference between stacked and unstacked states for an equimolar mixture of A and U (eq 4) and β is defined

$$\alpha = \frac{\epsilon(\nu)_{A,u} + \epsilon(\nu)_{U,u}}{2} - \epsilon(\nu)_{A\text{-}U} \quad (4)$$

as the normalized absorbance difference between stacked and unstacked G and C (eq 5).

$$\beta = \frac{\epsilon(\nu)_{G,u} + \epsilon(\nu)_{C,u}}{2} - \epsilon(\nu)_{G\text{-}C} \quad (5)$$

Equation 3 is a linear equation of the form $y = b + mx$ from which the *fraction* of paired A's in the RNA is equal to b (i.e., the y intercept) and the *fraction* of paired G's is equal to m (i.e., the slope). The *number* of paired A's (or G's) is obtained by multiplying $f_{A,s}$ (or $f_{G,s}$) by the total number of bases in the RNA (e.g., 121 for *S. carlsbergensis* 5S RNA).

Materials and Methods

Isolation and Purification of 5S RNA. Yeast (*S. carlsbergensis*) cell paste was extracted in 300–400-g quantities for 2 h at room temperature in the presence of sodium dodecyl sulfate (SDS) and phenol (Rubin, 1975). The aqueous phase was extracted with phenol a second time, followed by precipitation of the aqueous phase with 2 volumes of cold (−20 °C) 95% ethanol. The ethanol precipitate was dissolved in 1.2 M NaCl, 10 mM $MgCl_2$, and 10 mM tris(hydroxymethyl)aminomethane hydrochloride (Tris-HCl), pH 7.5, and heated to 65 °C for 10 min. After this cooled slowly to room temperature, a trace of undissolved material was removed by centrifugation at 10000*g* for 10 min. The supernatant was diluted with 10 mM $MgCl_2$–10 mM Tris-HCl, pH 7.5, to give a NaCl concentration of 0.3 M.

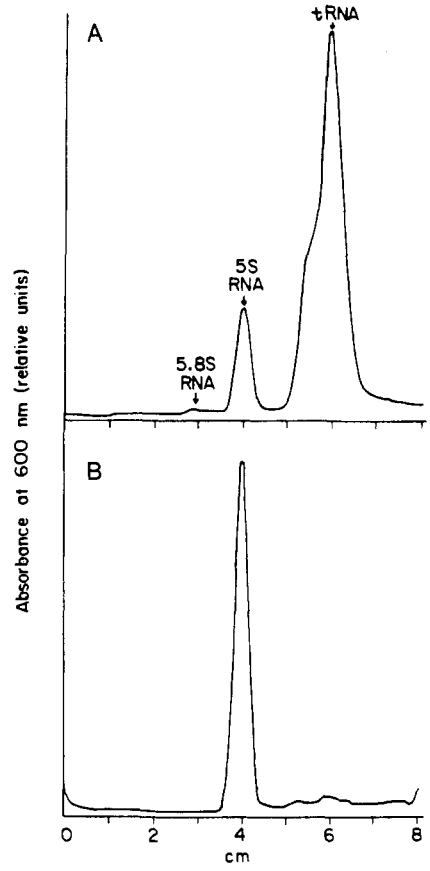

FIGURE 1: Polyacrylamide slab gel electrophoresis profiles of yeast 5S RNA before (A) and after (B) Sephadex G-75 chromatography, demonstrating the removal of contaminating tRNA and high molecular weight RNAs.

This RNA/protein solution was applied to a DEAE-cellulose (Whatman DE-32) column previously equilibrated with 0.3 M NaCl, 10 mM $MgCl_2$, and 10 mM Tris-HCl, pH 7.5. After the application of the sample, the column was washed with the same buffer until the effluent A_{260} was <0.1, indicating that the remaining protein had been removed. RNA was then eluted from the column with 1.0 M NaCl, 10 mM $MgCl_2$, and 10 mM Tris-HCl, pH 7.5, and precipitated with 2 volumes of cold 95% ethanol.

5S RNA was separated from trace amounts of large ribosomal RNA (28 S, 18 S, 5.8 S) and a large amount of mixed tRNAs by large-scale (5 × 150 cm column) gel permeation chromatography with Sephadex G-75 (fine) previously equilibrated in 1.0 M NaCl, 10 mM $MgCl_2$, and 10 mM Tris-HCl, pH 7.5.

Purity of the 5S RNA preparation was demonstrated (see Figure 1) by polyacrylamide slab gel electrophoresis (Maxam & Gilbert, 1980) on 8% denaturing gels. Absence of nicks was further evident by the complete absence of any signal at 20 ppm from phosphoric acid in a ^{31}P FT-NMR spectrum (not shown). The final yield of pure 5S RNA was about 10 mg/100 g of yeast cell paste used for the initial extraction.

Preparation of IR "Reference" Standards. Ribonucleotide phosphates (5′-GMP, 5′-CMP, 5′-AMP, and 5′-UMP) were purchased from P-L Biochemicals and used without further purification. The double-stranded polyribonucleotides [poly(rG)·poly(rC) and poly(rA)·poly(rU)] were prepared according to the method of Lafleur et al. (1972), using poly(rG), poly(rC), poly(rA), and poly(rU) from P-L Biochemicals. After formation, the double-stranded complexes were precipitated with 95% ethanol, lyophilized, and stored at −20 °C.

Measurement of Ribonucleic Acid Concentration. Aliquots of original stock solutions of ribonucleic acids were hydrolyzed in 0.3 M NaOH at 37 °C for 18 h. The molar concentration of nucleotide in each digest was calculated by using published extinction coefficients (Dawson et al., 1969) at 260 nm for the 5′-phosphates in alkaline solution and expressed as moles of phosphate. *S. carlsbergensis* 5S RNA concentration (as moles of phosphate residues after alkaline hydrolysis) was determined by using an extinction coefficient of 10 450 M^{-1} cm^{-1} computed from the published extinction coefficients for the component 5′-phosphates and the known primary sequence of *S. carlsbergensis* (b) (Erdmann, 1982).

Preparation of Ribonucleic Acids for FT-IR Spectrometry. Yeast 5S RNA samples in the absence of $MgCl_2$ were prepared by dissolving the RNA in 10 mM sodium cacodylate, pH 7.0, 10 mM ethylenediaminetetraacetic acid (EDTA), and 100 mM NaCl and heating the solution to 65 °C for 5 min. After slowly cooling to room temperature, the 5S RNA solution was dialyzed for 24 h at 8 °C against 1000 volumes of 10 mM sodium cacodylate, pH 7.0, and 100 mM NaCl. After dialysis, the 5S RNA was precipitated with 95% ethanol and lyophilized twice from a 99.8% deuterium oxide solution. For FT-IR measurements, the 5S RNA was dissolved in 10 mM sodium cacodylate, pH meter reading 7.0, 100 mM NaCl, in 99.8% D_2O. Yeast 5S RNA samples in the presence of $MgCl_2$ were prepared by using the same procedure except that the first step (heating to 65 °C in the presence of EDTA) was omitted and 10 mM $MgCl_2$ was included in all buffers. The final 5S RNA concentration was 25–30 mg/mL (0.08–0.09 M expressed as moles of phosphate per liter).

Poly(rG)·poly(rC) and poly(rA)·poly(rU) were twice lyophilized from 99.8% D_2O solution. For FT-IR measurements, these double-stranded polymers were dissolved in 10 mM sodium cacodylate, pH meter reading 7.0, 100 mM NaCl, in 99.8% D_2O. The 5′-phosphates were dissolved directly in the same buffer. The final concentrations of these standard compounds ranged from 0.06 to 0.07 mol of phosphate/L.

Fourier-Transform Infrared Spectrometry. The infrared absorption spectra of yeast 5S RNA and standard ribonucleotides were measured at 2-cm^{-1} resolution in cells with CaF_2 windows and 0.044-mm path length. Yeast 5S RNA spectra at elevated temperatures were obtained by wrapping the stainless steel cell holder with coils of nichrome wire connected to a DC power supply. Asbestos tape was used to insulate the nichrome wire. Spectra of the 5′-mononucleotide and double-stranded polyribonucleotides were measured at 25 °C. Sample temperature was determined by using a calibrated iron–constantan thermocouple attached directly to the infrared cell.

Spectra in the 1000–4000-cm^{-1} region were detected with a Digilab FTS-14D interferometer fitted with a standard triglycine sulfate pyroelectric detector. For each sample, 256 digitized interferograms were accumulated and then Fourier transformed to give a single-beam spectrum. A single-beam reference spectrum was acquired from 10 mM sodium cacodylate, pH meter reading 7.0, 100 mM NaCl, in 99.8% D_2O.

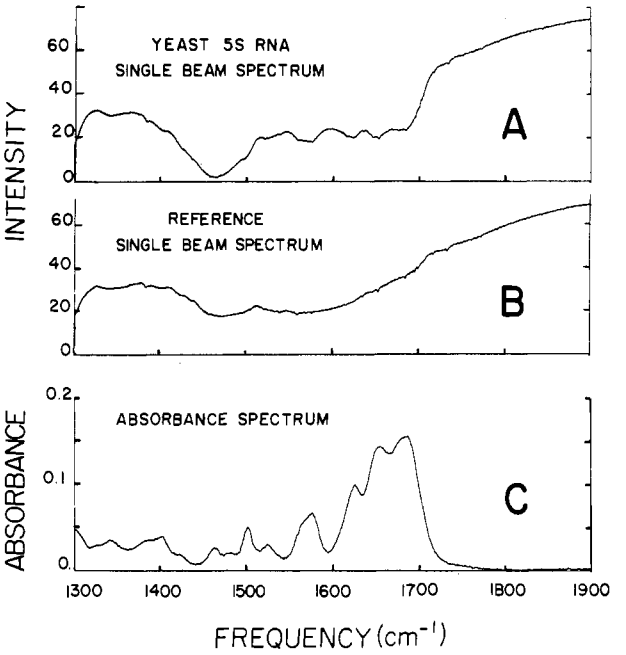

FIGURE 2: Generation of FT-IR absorbance spectrum for yeast 5S RNA (C) from single-beam transmittance spectra of yeast 5S RNA solution (A) and buffer (B). Each absorbance data point, $A(\nu)$, in (C) is obtained from $A(\nu) = \log [T(\nu)_{buffer}/T(\nu)_{RNA}]$, in which $T(\nu)_{RNA}$ and $T(\nu)_{buffer}$ are the transmittances from (A) and (B). The small spikes visible in (A) and (B) arise from water vapor due to incomplete purging of the spectrometer; any residual spikes remaining in the absorbance spectrum are easily recognized and have been removed by absorbance subtraction. Finally, different HDO concentrations in sample and buffer [compare 1457-cm^{-1} regions in (A) and (B)] would produce an interfering absorbance band in (C). That interference has been removed by absorbance subtraction, by using an HDO absorbance spectrum obtained by ratioing transmittance spectra from 99.8% and 97.3% D_2O solutions at that temperature.

Each absorbance spectrum was computed from the logarithm of the ratio of the single-beam sample and reference spectra, both measured at the same temperature, as illustrated in Figure 2. Absorbance spectra were corrected for small differences in water vapor content (due to slight differences in purging the sample compartment) and for small differences in HDO content in the sample and reference buffers, as described in the legend for Figure 2.

Results and Discussion

Figure 2 shows the generation of a typical Fourier-transform infrared absorbance spectrum from single-beam transmittance spectra for sample and buffer. Signal-to-noise ratio in the data may be enhanced by accumulating and adding many interferograms before calculating single-beam spectra, which are ratioed to produce the final absorbance spectrum. Moreover, from separate measurement of the spectrum of water vapor, the small spikes due to water vapor are readily removed by digital subtraction. Finally, the correction of the base line for small differences in HDO concentration (which can lead to large distortion in the base line) is easily carried out as described in the figure legend. The resulting absorbance spectrum is then converted to an extinction coefficient spectrum as described under Materials and Methods. All reported spectra are plotted directly from computer memory and have not been traced or smoothed in any way. FT-IR reference spectra for each of the four ribonucleotide 5′-phosphates are qualitatively similar to those originally obtained from a dispersive instrument (Thomas, 1969) but with much-improved signal-to-noise ratio and flatter base line, even at such small absorbance values.

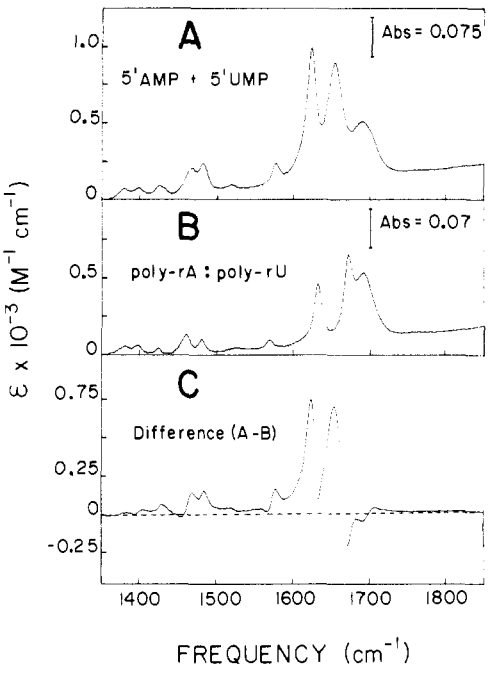

FIGURE 3: Determination of infrared extinction coefficient vs. frequency for A-U base pairs. (A) Spectrum consisting of half the sum of the spectra of 5'-AMP and 5'-UMP. (B) Spectrum for double-stranded poly(rA)·poly(rU). (C) Difference spectrum, (A) − (B), representing the infrared spectrum of an A-U base pair. All extinction coefficients are normalized per mole of phosphate (see text).

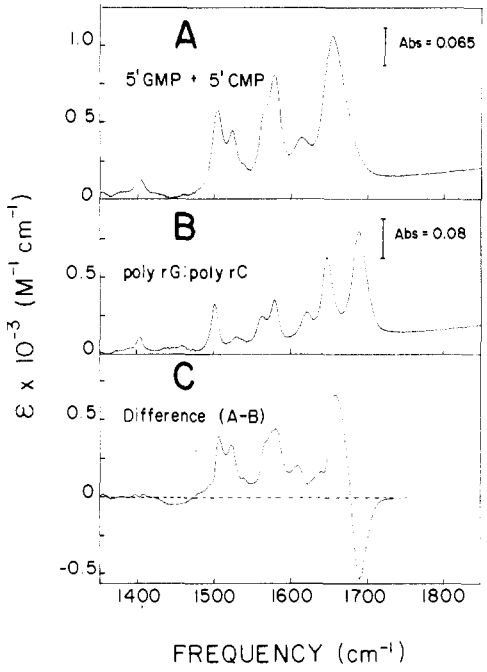

FIGURE 4: Determination of infrared extinction coefficient vs. frequency for G-C base pairs. (A) Spectrum consisting of half the sum of the spectra of 5'-GMP and 5'-CMP. (B) Spectrum for double-stranded poly(rG)·poly(rC). (C) Difference spectrum, (A) − (B), representing the infrared spectrum of a G-C base pair. All extinction coefficients are normalized per mole of phosphate (see text).

Figure 3 shows the infrared spectra for unpaired (A) and paired (B) A and U. The difference spectrum, (A) − (B), is taken to represent the infrared extinction due to A-U base pairs. Figure 4 shows similar spectra for G-C pairs. At this stage, it may be worth collecting the assumptions upon which the present data reduction is based: (i) All RNA bases are either paired or unpaired. In other words, no intermediate states (e.g., "frayed ends" in helical segments) are permitted.

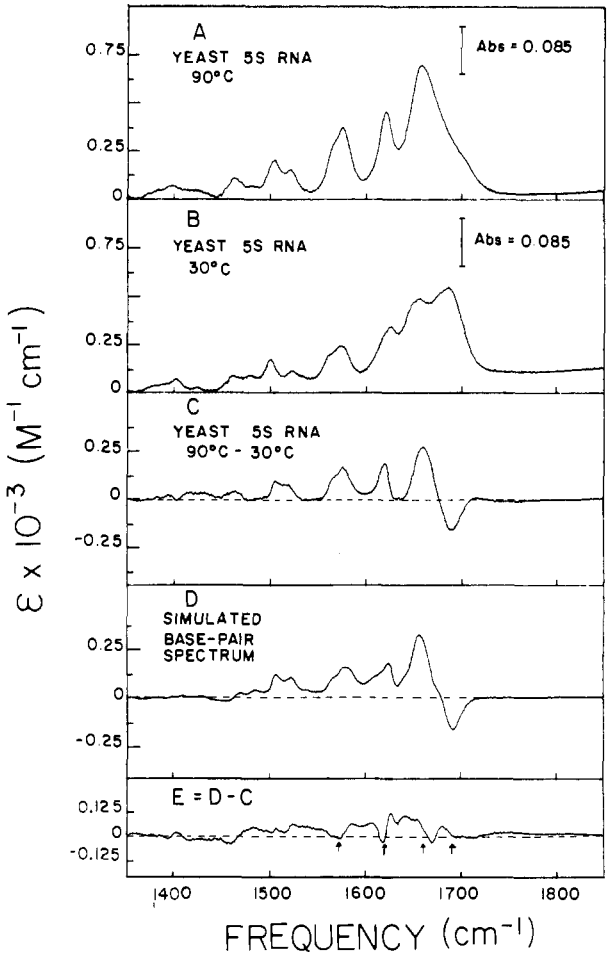

FIGURE 5: Infrared spectra of yeast 5S RNA in the absence of Mg^{2+}. (A) Infrared spectrum of yeast 5S RNA at 90 °C, for which all bases are assumed to be unstacked. (B) Infrared spectrum of yeast 5S RNA at 30 °C, for which all bases are assumed to be stacked in the native conformation. (C) Difference spectrum, (A) − (B), representing the infrared intensity due to stacking of the RNA bases. (D) Simulation of (C), computed from the best fit linear combination of Figures 3C and 4C, in a proportion determined from $f_{s,A}$ and $f_{s,G}$ of Figure 7A (see text). (E) Difference spectrum, (D) − (C), representing the difference between experimental and simulated base-pair content. Arrows denote positions of maximum intensity in (C).

(ii) There are only two possible types of base pairs, A-U and G-C (e.g., no G-U pairs). (iii) Base stacking in single-stranded RNA segments is ignored—in other words, the difference spectra in Figures 3C, 4C, 5C, and 6C represent A-U and G-C base pairs only. (iv) At 30 °C, all base pairs in the native yeast 5S RNA conformation are present. (v) At 90 °C, all bases in yeast 5S RNA are completely unstacked and unpaired. (vi) Any tertiary base pairs behave as Watson–Crick pairs.

The ultraviolet absorbance at either 260 or 280 nm of *S. cerevisiae* 5S RNA in the presence of Mg^{2+} shows no change below 30 °C or above about 88 °C; in the absence of Mg^{2+}, A_{260} is constant above about 70 °C and changes by less than 8% below 30 °C (Luoma et al., 1980). Since the primary sequences of *S. cerevisiae* and *S. carlsbergensis* are identical (Erdmann, 1982), it is reasonable to conclude that above-stated assumptions iv and v are valid. The FT-IR spectra in Figure 5A,B (or 6A,B) thus correspond to native (30 °C) and heat-denatured (90 °C) *S. carlsbergensis* 5S RNA in the absence (or presence) of Mg^{2+}. The difference spectrum between native and denatured forms (Figure 5C or 6C) is is then a measure of base stacking and base pairing in yeast 5S RNA.

The remaining question is how to quantify the numbers of

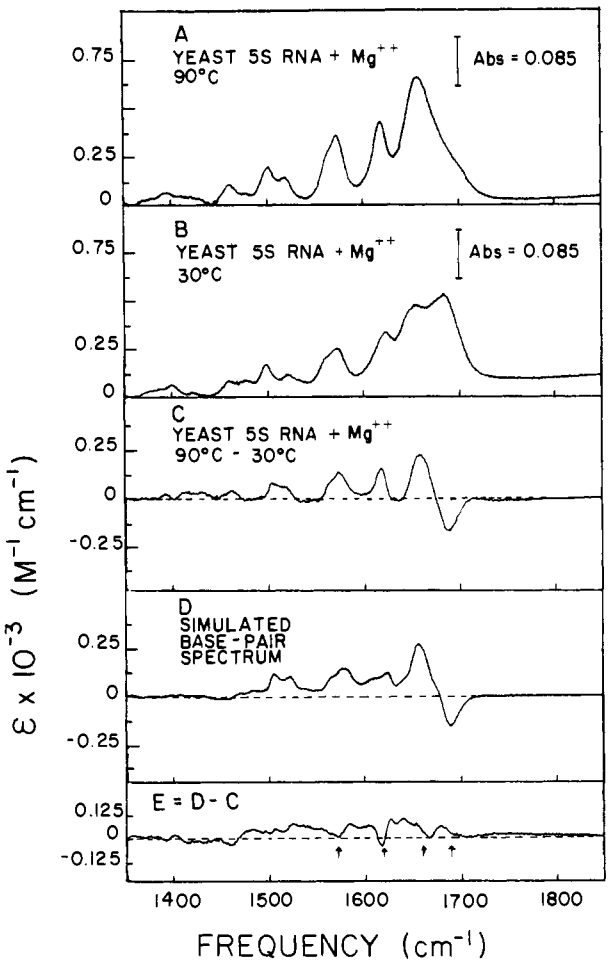

FIGURE 6: Infrared spectra of yeast 5S RNA in the presence of Mg^{2+}. (A)–(C) and (E) are as in Figure 5. (D) Simulation of (C), computed from the best fit linear combination of Figures 3C and 4C, in a proportion determined from $f_{s,A}$ and $f_{s,G}$ of Figure 7B (see text).

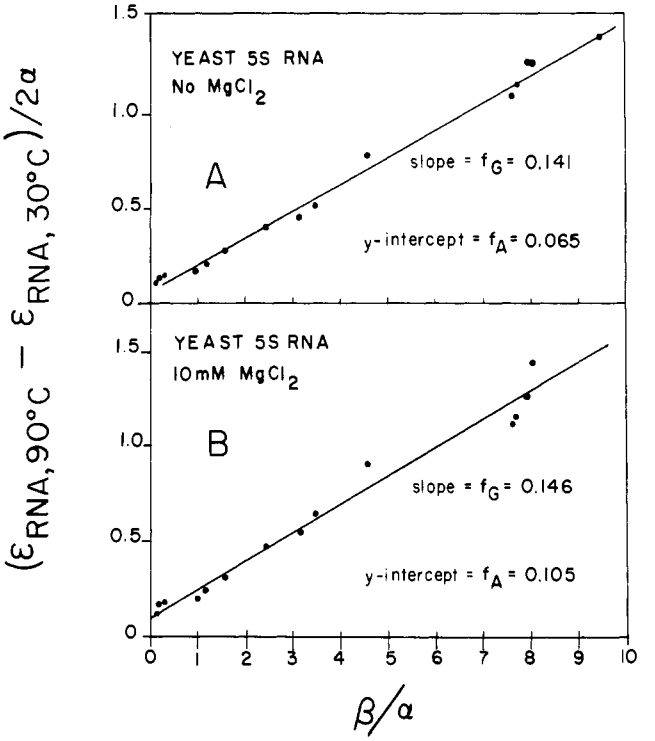

FIGURE 7: Determination of base-pair composition of yeast 5S RNA from infrared spectral intensity data. Data are reduced according to eq 3, from IR intensity data distributed within ±5 cm^{-1} of the four largest peaks in the difference spectra of Figures 5C and 6C (see text). The straight line is a least-squares best fit. The y intercept, $f_{s,A}$, is the number of stacked A residues as a fraction of the total number of bases in the RNA. The slope, $f_{s,G}$, is the number of stacked G residues as a fraction of the total number of bases in the RNA. Equation 3 is based on the assumption that all stacked bases are paired: i.e., $f_{s,A} = f_{s,U}$ and $f_{s,G} = f_{s,C}$. (A) No Mg^{2+}; (B) 10 mM Mg^{2+}.

Table I: Number of Base Pairs in Yeast 5S RNA

technique	$-Mg^{2+}$	$+Mg^{2+}$	ref
FT-IR	17 (G-C)	18 (G-C)	this work
	8 (A-U)	13 (A-U)	
	25 (total)	31 (total)	
dispersive IR		24 (G-C)	Stulz et al., 1981
		22 (A-U)	
		46 (total)	
Raman		⩽17 (G-C)	Luoma &
		⩽18 (A-U, G-U)	Marshall, 1978b
		⩽35 (total)	
UV		⩽24 (G-C)	Luoma et al.,
hypochromism		⩽16 (A-U)	1980
	⩽36 (total)	⩽40 (total)	
^1H FT-NMR	⩾27 (total)		this work; unpublished results

A-U and G-C base pairs represented in Figure 5C. Although the spectra of appropriately prepared 1:1 mixtures of poly(rA)·poly(rU) (Figure 3B) and poly(rG)·poly(rC) (Figure 4B) probably give accurate descriptions of A-U pairs and G-C pairs, it is not so easy to provide accurate models for unpaired A, C, G, and U bases. For example, the heat-denatured homopolymers are not suitable—poly(rG) exhibits some residual base stacking even at 90 °C, as evidenced by its UV absorption vs. temperature profile. We have therefore chosen the mononucleotide 5′-phosphates as reference spectra to represent unpaired nucleotide bases in RNA.

Equation 3 expresses two unknowns, $f_{A,s}$ and $f_{G,s}$, in terms of three observables, $[\epsilon(\nu)_{RNA,90°C} - \epsilon(\nu)_{RNA,30°C}]/2$, α, and β. Since the total number of nucleotides in the primary RNA sequence is 121 (Erdmann, 1982), the FT-IR extinction coefficients at two wavelengths would suffice to determine the number of A-U pairs and G-C pairs (namely, $121f_{A,s}$ and $121f_{G,s}$, respectively). Obviously, the accuracy of the determination will be improved by using FT-IR intensity data at more than two wavelengths. Figure 7 provides simple graphical determinations of $f_{A,s}$ and $f_{G,s}$, on the basis of a linear least-squares best fit straight line through the data. In order to improve precision without introducing bias in the selection of data points, equally spaced points were chosen within ±5 cm^{-1} of the four largest peaks in the difference spectra of Figures 5C and 6C. The best fit values of $f_{A,s}$ and $f_{G,s}$ from Figure 7 were then used to construct corresponding linear combinations of the spectra in Figures 3C and 4C to give simulated "base-pair spectra" (Figures 5D and 6D) for comparison to the observed RNA base-pair spectra of Figures 5C and 6C. In spite of the various approximations involved, simulated and experimental base-pair spectra agree to within approximately 10%, as judged by the difference spectrum between them (Figures 5E and 6E). The base-pair numbers determined from Figure 7 are listed in Table I, along with values determined by other techniques.

Only the proton NMR experiment detects base *pairs*; the various optical methods detect base *stacking* and thus tend to *overestimate* the number of base pairs (Tsuboi et al., 1973). On the other hand, lability of the base-pair protons with respect to exchange with solvent H_2O can broaden or eliminate proton NMR signals; thus, the proton NMR base-pair estimates

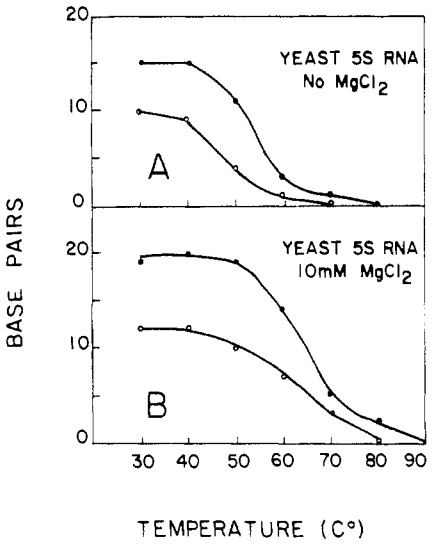

FIGURE 8: Number of yeast 5S RNA A-U (○) and G-C (●) base pairs as a function of temperature. Base-pair numbers were determined from eq 3, from FT-IR intensity data at 1620 and 1575 cm^{-1}. (A) No $MgCl_2$; (B) 10 mM $MgCl_2$.

Table II: Midpoints of Temperature-Induced Unfolding for Yeast 5S RNA

technique	$-Mg^{2+}$	$+Mg^{2+}$	ref
FT-IR	47 °C (A-U) 54 °C (G-C)	63 °C (A-U) 65 °C (G-C)	this work
UV hypochromism	48 °C	66 °C	Luoma et al., 1980
CD	≥52 °C	≥64 °C	Luoma et al., 1980
ESR		57 °C	Luoma et al., 1982

represent a *minimum* base-pair number. The base-pair determinations from previously published Raman (Luoma & Marshall, 1978b) and our own preliminary 500-MHz proton FT-NMR spectra thus provide limits of 27 (lower limit, in the absence of Mg^{2+}) to 35–40 (upper limit, in the presence of Mg^{2+}), consistent with the present determinations of 25 ± 3 and 31 ± 3 total base pairs in the absence or presence of Mg^{2+}. A previous IR determination (Stulz et al., 1981) of 46 total base pairs in the presence of Mg^{2+} is clearly too high for the reasons explained in the introduction. The only technique that can unambiguously detect G-U pairs is proton NMR homonuclear Overhauser enhancement (Hare & Reid, 1982; Roy et al., 1982; Heerschap et al., 1982); such studies are currently in progress in our laboratory.

The base-pair spectrum simulation is most accurate, as might be expected, at the centers of the four largest peaks in the difference spectrum (see arrows in Figures 5E and 6E). Therefore, for temperature-denaturation studies, $f_{A,s}$ and $f_{G,s}$ were determined from eq 3 by using data from the two difference peak maxima at 1575 and 1620 cm^{-1}. The FT-IR melting profiles are displayed in Figure 8, and the melting midpoints are listed in Table II, for comparison with results from other methods.

The FT-IR melting midpoints are in excellent agreement with the UV hypochromism and circular dichroism values (Luoma et al., 1980) (ca. 50 °C in the absence of Mg^{2+} and 65 °C in the presence of Mg^{2+}). The electron spin resonance (ESR) melting curve shows a melting midpoint slightly lower than the optical measurements. Since the ESR rotational correlation time reflects motional flexibility at the labeled site (3′-terminus), whereas the optical intensity reflects the

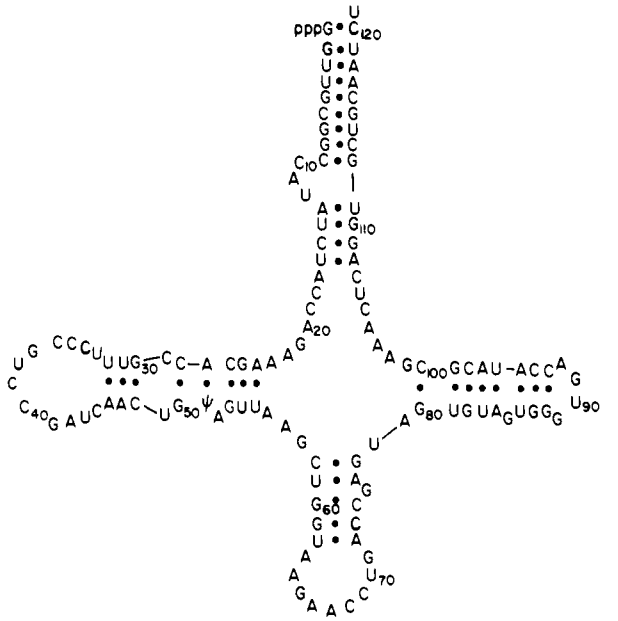

FIGURE 9: Proposed universal secondary base-pairing scheme for yeast 5S RNA (Luoma & Marshall, 1978b). The number and types of base pairs predicted by this model are in good agreement with the present FT-IR results (see Discussion).

equilibrium proportion of stacked and unstacked bases, it thus appears likely that the stem base pairs begin to flex (ca. 57 °C) before they begin to break (65 °C).

Figure 9 shows one of the many proposed secondary base-pairing models for eukaryotic 5S RNAs (Luoma & Marshall, 1978b). An attractive feature of this particular model is that it can be adapted to all published prokaryotic, eukaryotic, and archebacterial 5S RNA sequences, as well as to eukaryotic 5.8S RNA (Luoma & Marshall, 1978a,b; G. A. Luoma and A. G. Marshall, unpublished work). Of the 34 possible base pairs predicted by the model, 16 are G-C, 13 are A-U, and 5 are G-U. The model thus agrees very closely with the experimental values of 18 G-C and 13 A-U pairs determined by FT-IR in the presence of Mg^{2+}.

It is clear from comparison of panels C and D of Figure 5 (or 6) in regions (e.g., 1580–1610 and 1630–1650 cm^{-1}) between the largest difference peaks that the mononucleotide standards evidently do not completely represent unpaired bases in RNA. In other words, the individual bases in the denatured 5S RNA polymer do not behave independently as do the mononucleotides, due in part to residual base stacking in the denatured RNA. A second reason may be the presence in RNA of G-U pairs not present in the "standard" spectra. Although poly(rG) and poly(rU) do not by themselves pair up in solution, Stulz et al. (1981) have proposed using poly[r(A,G)]·poly(rU) and poly(rG)·poly[r(C,U)] in order to introduce some G-U pairs into otherwise "pure" A-U or G-C polymers for use as IR standards. However, their dispersive IR measurements were of insufficient accuracy for useful quantitation of RNA base pairing. In future, it should prove interesting to perform FT-IR measurements on such polymers to yield FT-IR standard spectra for G-U base pairs.

Acknowledgments

S. carlsbergensis cells were generously provided by the Anheuser-Busch Brewery in Columbus, OH. Major components of the infrared interferometer were made available (to J.O.A.) by Dr. Robert L. Berger, Chief, Biophysical Instrumentaton Section, Laboratory of Technical Development, NHLBI, National Institutes of Health.

Registry No. Mg, 7439-95-4; 5′-CMP, 63-37-6; 5′-UMP, 58-97-9; 5′-GMP, 85-32-5; 5′-AMP, 61-19-8.

References

Appel, B., Erdmann, V. A., Stulz, J., & Ackermann, Th. (1979) *Nucleic Acids Res. 7*, 1043–1057.

Böhm, S., Fabian, H., Venyaminov, S. Y., Matveev, S. V., Lucius, H., Welfle, H., & Filimonov, V. V. (1981) *FEBS Lett. 132*, 357–361.

Burns, P. D., Luoma, G. A., & Marshall, A. G. (1980) *Biochem. Biophys. Res. Commun. 96*, 805–811.

Carey, P. R. (1982) *Biochemical Applications of Raman and Resonance Raman Spectroscopies*, Chapter 7, pp 184–207, Academic Press, New York.

Chen, M. C., Giege, R., Lord, R. C., & Rich, A. (1978) *Biochemistry 17*, 3134–3138.

Dawson, R. M. C., Elliott, D. C., Elliott, W. J., & Jones, K. M., Eds. (1969) in *Data for Biochemical Research*, 2nd ed., pp 169–179, Oxford University Press, Oxford.

Erdmann, V. A. (1976) *Prog. Nucleic Acid Res. Mol. Biol. 18*, 45–90.

Erdmann, V. A. (1982) *Nucleic Acids Res. 10*, r93–r105.

Hare, D. R., & Reid, B. R. (1982) *Biochemistry 21*, 5129–5135.

Heerschap, A., Haasnoot, C. A. G., & Hilbers, C. W. (1982) *Nucleic Acids Res. 10*, 6981–7000.

Ladner, J. E., Jack, A., Robertus, J. D., Brown, R. S., Rhodes, D., Clark, B. F. C., & Klug, A. (1975) *Proc. Natl. Acad. Sci. U.S.A. 72*, 4414–4418.

Lafleur, L., Rice, J., & Thomas, G. J., Jr. (1972) *Biopolymers 11*, 2423–2437.

Luoma, G. A., & Marshall, A. G. (1978a) *Proc. Natl. Acad. Sci. U.S.A. 75*, 4901–4905.

Luoma, G. A., & Marshall, A. G. (1978b) *J. Mol. Biol. 125*, 95–105.

Luoma, G. A., Burns, P. D., Bruce, R. E., & Marshall, A. G. (1980) *Biochemistry 19*, 5456–5462.

Luoma, G. A., Herring, F. G., & Marshall, A. G. (1982) *Biochemistry 21*, 6591–6598.

Maxam, A., & Gilbert, W. (1980) *Methods Enzymol. 65*, 499–560.

Reid, B. R., & Robillard, G. T. (1975) *Nature (London) 257*, 287–291.

Richards, E. G., Geroch, M. E., Simpkins, H., & Lecanidou, R. (1972) *Biopolymers 11*, 1031–1039.

Roy, S., Papastavros, M. Z., & Redfield, A. G. (1982) *Biochemistry 21*, 6081–6088.

Rubin, G. M. (1975) *Methods Cell Biol. 12*, 45–64.

Schernau, U., & Ackermann, Th. (1977) *Biopolymers 16*, 1735–1745.

Stulz, J., Ackermann, Th., Appel, B., & Erdmann, V. A. (1981) *Nucleic Acids Res. 9*, 3851–3861.

Sussmann, J. L., & Kim, S. H. (1976) *Biochem. Biophys. Res. Commun. 68*, 89–96.

Thomas, G. J., Jr. (1969) *Biopolymers 7*, 325–334.

Tsuboi, M., Takahasi, S., & Harada, I. (1973) in *Physio-Chemical Properties of Nucleic Acids*, pp 91–145, Academic Press, New York.

Inactivation of Yeast Hexokinase B by Triethyltin Bromide†

Kevin R. Siebenlist and Fumito Taketa*

ABSTRACT: Triethyltin bromide was found to demonstrate temperature-dependent inactivation of yeast hexokinase B. At temperatures of 20 °C or lower, little or no inactivation of the enzyme was detected after 2 h of reaction with 50–300 μM concentrations of the reagent. However, incubation at 25 °C or higher resulted in an increased rate and extent of loss of the enzyme activity with increasing incubation temperatures. The Arrhenius plot for the inactivation process showed a sharp break at approximately 30 °C, with a heat of activation (ΔH^*) above this temperature of 55.2 kcal, indicating that a triethyltin-induced conformational change occurred at the elevated temperatures. Sugar substrates provided protection against the inactivating effect by reducing the binding of triethyltin to the enzyme. In the absence of glucose, two sites of different affinity for triethyltin exist in the hexokinase monomer. Binding of triethyltin to the enzyme shifted its monomer–dimer equilibrium toward the monomeric form in an early stage of the interaction. Inactivation of the enzyme was associated with a slower subsequent event. Comparative effects of various organotin compounds on the activity of the enzyme indicated that inhibitory potency was associated with increasing hydrophobicity of the alkyl groups attached to the tin.

Hexokinase (ATP:D-hexose 6-phosphotransferase, EC 2.7.1.1) is the first enzyme of the glycolytic pathway and, as such, is of critical importance to the overall energy-producing metabolism of the cell. The enzyme isolated from yeast exists as two noninterconvertible isoenzymes, A and B, which at neutral pH are predominantly dimers of molecular weight 102 000, that can be dissociated into identical monomers by increasing the pH or the ionic strength of the medium (Schultze & Colowick, 1969; Derechin et al., 1972; Easterly & Rosemeyer, 1972). In addition to its hexose phosphorylating activity, yeast hexokinase has an ATPase activity that is 5 orders of magnitude lower that can be stimulated 20-fold by addition of lyxose or xylose, nonphosphorylatable analogues of the sugar substrates (Dela Fuente et al., 1970). The lyxose stimulation of ATPase activity of the hexokinase is reportedly due to the fit of this pentose in the hexose binding site which induces a conformational change in the enzyme from a

† From the Department of Biochemistry, Medical College of Wisconsin, Milwaukee, Wisconsin 53226. *Received March 18, 1983.* This work was supported by National Institute of Arthritis, Metabolic and Digestive Diseases Grant AM-15770.

0006-2960/83/0422-4229$01.50/0